Title
Characterization of Nontoxic Liquid-Metal Alloy Galinstan for Applications in Microdevices

Journal
Journal of Microelectromechanical Systems, 21(2)

ISSN
1057-7157

Authors
Liu, Tingyi
Sen, Prosenjit
Kim, Chang-Jin

Publication Date
2012-04-01

DOI
10.1109/jmems.2011.2174421

Peer reviewed

Authors' final manuscript for: J. MICROELECTROMECHANICAL SYSTEMS, VOL. 21, NO. 2, APRIL 2012, pp. 443-450.

Characterization of Nontoxic Liquid-Metal Alloy Galinstan® for Applications in Microdevices

Tingyi "Leo" Liu, Prosenjit Sen and Chang-Jin "CJ" Kim

Mechanical and Aerospace Engineering Department

University of California, Los Angeles (UCLA), CA 90095, USA

Abstract— We have obtained interfacial properties of Galinstan®, a nontoxic liquid-metal alloy, to help replace mercury in miniature devices. To prevent formation of an oxide skin that severely hinders the fluidic behavior of small Galinstan® droplets and leads to inaccurate property data, we performed our experiments in a nitrogen-filled glove box. It was found that only if never exposed to oxygen levels above 1 parts-per-million (ppm) would Galinstan® droplets behave like a liquid. Two key properties were then investigated: contact angles and surface tension. Advancing and receding contact angles of Galinstan® were measured from sessile droplets on various materials: for example, 146.8º and 121.5º, respectively, on glass. Surface tension was measured by the pendant drop method to be 534.6±10.7 mN/m. All the measurements were done in nitrogen at 28ºC with oxygen and moisture levels below 0.5 ppm. To help design droplet-based microfluidic devices, we tested the response of Galinstan® to electrowetting-on-dielectric (EWOD) actuation.

Index Terms— liquid-metal, Galinstan®, Galinstan® oxidation, Galinstan® contact angle, Galinstan® surface tension, electrowetting-on-dielectric (EWOD)

This work was supported by DARPA HERMIT program.

T. Liu and C.-J. Kim are with the Mechanical and Aerospace Engineering Department, University of California, Los Angeles (UCLA), CA 90095, USA. (e-mail: leolty@ucla.edu; Phone: 310-825-3977)

P. Sen is currently with Innovative Micro Technology (IMT), Santa Barbara, CA 93117, USA.

I. INTRODUCTION

For the excellent conductivities of a metal and the fluidic properties of a liquid, metals are often employed in their liquid state: mercury, gallium (alloy), aluminum, and tin, etc. At room temperature, however, the choice is significantly limited; mercury, used commonly for thermometers and electromechanical relays, remains the only liquid metal as an element. Gallium and many of its alloys are a liquid near but above room temperature. Although some laboratories may have produced some in-house, a room-temperature liquid metal has not become available until recently. Galinstan®, an alloy of 68.5% Ga, 21.5% In, and 10.0% Sn, is a commercially available (from Geratherm® Medical AG in Germany and distributed by RG Medical Diagnostics in USA) nontoxic liquid-metal that replaces mercury mostly in thermometers [1]. Physical properties of Galinstan® and mercury [1, 2] are summarized in Table I for comparison. Like mercury, Galinstan® retains its liquid state well below 0ºC. Its nontoxic nature and ultra low vapor pressure ($<10^{-6}$ Pa at 500°C) make Galinstan® a better substitute for mercury in many liquid-metal applications, e.g. electromechanical relays [3], coolants [4], and ion sources [5]. In microelectromechanical systems (MEMS), Galinstan® has already been used [6, 7] or is in line to replace mercury [8, 9]. It has, however, failed to produce many successful results in MEMS as initially anticipated, and mercury is still the common choice of liquid metal in research at room temperature. The main reason for the slow adoption in micro devices is the fast oxidation of Galinstan®, as it was for gallium [10], making any study or development involving Galinstan® below millimeters difficult. In addition, several parameters important for microdevices are unavailable for this relatively new material. Even worse, some information available on the Internet (e.g., that Galinstan® wets glass) lacks rigor and often misleads.

Due to the dominance of the capillary effect at microscale, contact angles and surface tension are two key properties of a liquid used in MEMS, especially the droplet-based micro devices. For Galinstan®, however, no systematic study on contact angles has so far been reported, and surface tension data is either limited (from Geratherm® Medical AG in Germany [1]) or scattered (between 0.501 N/m and 0.718 N/m [11, 12]) in the literature. The major challenge of characterizing Galinstan® lies in the fact that its surface oxidizes instantaneously in air. The oxidation effect is rather profound at microscale, where the surface-to-volume ratio is large, making small droplets of Galinstan® behave like a gel rather than a normal liquid. To obtain genuine properties not obscured by the surface oxidation, we performed all the tests in this report inside a glove box of high-purity inert environment. Keeping Galinstan® free of oxidation will stay as a main issue in developing micro devices that involve free surfaces of Galinstan®.

II. THEORIES

A. Contact Angle Measurements

The contact angle is an experimentally observable quantity that describes the wetting property of a liquid in contact with a solid surface and surrounded by another immiscible fluid (most commonly a gas), as shown in Fig. 1(a). This macroscale measurement ignores the nanoscopic region where molecular interaction between the phases (i.e. liquid, gas, and solid) is significant. Intrinsic contact angle free of hysteresis is expected only on an ideal solid surface, while in reality the contact angle of an advancing meniscus exceeds that of a receding meniscus. The advancing and receding contact angles define the upper and lower limits of the contact angle of a static liquid, and their difference is referred to as contact angle hysteresis. Since deviations from the ideal surface, such as roughness and chemical inhomogeneity, are believed to cause the hysteresis and affect its magnitude, complete contact angle data should include information about the solid surface as well. As the surface cleanliness (chemical homogeneity) can be reasonably well maintained, in this report we measure roughness of the solid surface along with the contact angles.

B. Surface Tension Measurement

The surface tension of a liquid is the boundary tension at the interface between a liquid and an immiscible fluid (e.g. gas) due to the unbalanced molecular attraction from two sides of the interface. Because it is vital information in any capillary study, a series of methods of measuring surface tension have been established, among which the du Noüy ring method (e.g. du Noüy ring tensiometer), Wilhelmy slide method (e.g. Wilhelmy plate tensiometer), and pendant/sessile drop method (goniometer) are most widely used. For surface tension measurement of molten metals, in particular, the maximum bubble pressure method is also favored as well as the pendant/sessile drop method [13]. Considering the limited space inside a glove box to handle Galinstan® and perform the entire measurement, we have excluded the du Noüy ring method and Wilhelmy slide method. Also excluded was the maximum bubble pressure method, which requires precise pressure measurement equipment and a tank of Galinstan®. In contrast, the pendant/sessile drop method uses a simple optical system (i.e. light source and camera with pendant/sessile drop in-between) and only a few microliters of sample liquid (< 2 μL in our case).

The pendant/sessile drop method extracts the surface tension from the shape of the drop when the forces due to gravity and surface tension are comparable. Following the Young-Laplace equation, the pressure difference across a meniscus (liquid-air interface) is given by

$$\Delta p = \gamma\left(\frac{1}{R_1}+\frac{1}{R_2}\right) \tag{1}$$

where γ is the surface tension and $(1/R_1 + 1/R_2)$ is twice the mean curvature of the free surface. Note that R_1 and R_2 are not necessarily the principal radii of curvature as long as their planes are mutually orthogonal [13]. As a pendant/sessile drop is axisymmetric, the two radii of curvature R_1 and R_2 are equal, i.e., $R_1 = R_2 = R$, at the apex. Placing the coordinate origin at the apex as

seen in Fig. 1(b), pressure difference at the apex is given by $\Delta p(0) = 2\gamma/R$. Hydrostatic pressure due to gravity will distort the shape of the drop, resulting in a pressure difference at height z from the apex to be

$$\Delta p(z) = \Delta p(0) - \Delta\rho g z = \frac{2\gamma}{R} - \Delta\rho g z \tag{2}$$

where $\Delta\rho = \rho_{\text{liquid}} - \rho_{\text{gas}}$ and g is the gravitational acceleration. Combining Eqs. 1 and 2 together yields

$$\gamma\left(\frac{1}{R_1} + \frac{1}{R_2}\right) = \frac{2\gamma}{R} - \Delta\rho g z \tag{3}$$

which will serve as the governing differential equation of the droplet profile after substituting R_1 and R_2 with the variables proper for the coordinate system of interest. However, there is no analytical solution to this differential equation, and only a numerical solution exists. Eq. 3 can be rewritten into a set of three arc-length based first order equations below

$$\begin{aligned} \frac{d\phi}{ds} &= \frac{2}{R} - \frac{\Delta\rho g z}{\gamma} - \frac{\sin\phi}{r} \\ \frac{dr}{ds} &= \cos\phi \\ \frac{dz}{ds} &= \sin\phi \end{aligned} \tag{4}$$

where s is the arc length and ϕ is the angle between the r axis and the tangent at a point on the meniscus (Fig. 1(b)). Using these equations one can generate a series of theoretical profiles of a pendant/sessile drop by varying surface tension γ and the radius at the apex R as two parameters. By comparing the data points obtained from experiment (i.e., drop profile on an image) to the theoretical profiles, the surface tension can be determined [14].

In practice, in an effort to reduce the time of calculation and comparison, initial values of surface tension (or a parameter involving surface tension, e.g. Bond number) and the radius at the apex are estimated using empirical tables or polynomials and two data points from the experimentally obtained droplet image (viz. the selected plane method [14, 15]). Then, an accurate value of surface tension is obtained by varying surface tension and radius at the apex around the initial estimated values to minimize the sum of squares of the normal distance between the experimental data and the theoretical profile. We avoided the more complex and detailed optimization process used by Lin *et al.* [14], which include two more variables to locate the actual location of the apex (r_0, z_0), by introducing a plumb bob in our experiment. The plumb bob reveals the true axis of symmetry and corrects the data before they are sent to the computer program for calculation.

III. EXPERIMENTAL PROCEDURE

A. Prevention of Oxidation

As soon as Galinstan® is exposed to ambient air, its surface gets oxidized instantaneously (well below 1 s), turning the color from a shiny silver into a dull grey. Such an oxide skin influences the behavior of microscale droplets significantly due to their large surface-to-volume ratio. Fig. 2 vividly illustrates the fast oxidation of a 2 mm diameter droplet of Galinstan® dispensed from a plastic pipette (Gilson PIPETMAN® P1000) in a mere 0.2% oxygen environment – 100 times less than in ambient air. The surface was already oxidized during the dispensing action (< 0.25 s), forming a droplet of a pronounced non-spherical shape. When dispensed in ambient air, Galinstan® was pinned at the pipette tip by instantaneous oxidation, requiring a tap to the pipette to free the droplet.

In order to prevent the oxidation, Galinstan® should be kept in an inert environment (e.g. nitrogen [16] or argon [17]) or covered by another aqueous solution (e.g. diluted HCl [11, 12]), similarly to other gallium alloys. Following the procedures described in [16], we purged a glove box (VAC 101965 with oxygen and moisture sensors) with pre-purified nitrogen (99.998%) and had the built-in purification system continue to absorb oxygen and moisture. In addition, we controlled the flow rate of nitrogen (or air in the highest oxygen level case) in order to observe the behavior of Galinstan® at different levels of oxygen. The summary of our observations is listed in Table II. Note that even at ~20 ppm (i.e. 0.002%) of oxygen, in which dispensed droplets displayed a spherical shape, the droplet behaved as if a gel droplet rather than a normal liquid droplet; it was easily distorted to an irreversible non-spherical shape, if shear was applied on the droplet. Only when the oxygen content was reduced to below 1 ppm (0.0001%) did Galinstan® behave like mercury or other normal liquids, recovering a spherical shape at the removal of external shear on the droplet. To ensure that Galinstan® is free of oxidation, all of our characterization measurements were performed in nitrogen with both oxygen and moisture content below 0.5 ppm. Also note that all the data in this report were collected at 28°C (measured by Ever-Safe N16B glass organic filled MCT classical thermometer).

B. Vibration Isolation

Both the contact angle measurements and the surface tension measurement in this report involve an image analysis at the interfaces. Therefore, accuracy of the measurement highly depends on the quality of the pictures. In order to capture clear pictures of sessile or pendant drops, many aspects should be considered and controlled well when designing the experiments, such as vibration, lighting, camera tilt, and pixel errors from small droplets. Vibration, which leads to a blurred droplet profile, would cause large errors. To eliminate the vibration, we have placed the entire experiment setup, except the backlight, on a vibration-isolation plate (Vistek™

VIP Series 320) inside the glove box, as shown in Fig. 3. The backlight used had a significantly larger beam width than the camera's field of view and hence did not require vibration isolation.

C. Contact Angle Measurements

Imitating the commercial instruments (e.g. First Ten Angstroms FTÅ200) which measure contact angles using drop shape analysis, we have developed a setup inside the glove box for contact angle measurements of Galinstan®, as schematically depicted in Fig. 3. A syringe with liquid-metal compatible needle (Hamilton 50 μL syringe 1705RN and removable needle 7770-02 RN NDL with inner diameter 0.41 mm) was used to generate sessile droplets of Galinstan® on various solid surfaces.

The experiments proceeded as follows. First, a captive Galinstan® drop was created as shown in Fig. 1(a) by dispensing it manually from a syringe through the needle. The droplet was made much larger than the needle tip to minimize the surface distortion by the tip [18]. Second, the sessile droplet was expanded or contracted by pumping the liquid in and out of the syringe continuously and slowly (~0.25 μL/s) to maintain quasi-static states, while recording the side views of the droplet with a video camera (Edmund Optics EO-0413C) in audio video interleave (AVI) file format at 28 frames per second. Slow pumping of Galinstan® was more difficult than aqueous solutions (e.g. water), because liquid-metals have much larger surface tension and do not wet the needle material. Fresh Galinstan® was used for every test to prevent potential contamination. Finally, after the experiment was done, the video was inspected frame-by-frame and advancing and receding contact angles were obtained from the snapshot right before the contact line moved.

We measured the contact angles of Galinstan® on several solid materials commonly used in micro devices. Among metals, almost all of which chemically react with gallium and gallium alloys [19], tungsten was chosen for its chemical resistance. Mica was chosen for their well-known surface smoothness, despite its rare use in MEMS. Methods of surface preparation for all the materials tested are summarized in Table III. After completing contact angle measurements, surface roughness was measured for all the tested materials using atomic force microscopy (AFM).

D. Surface Tension Measurement

For surface tension measurement by the pendant drop method, the testing material and its substrate were removed from the contact angle measurement setup of Fig. 3. Added, instead, was a plumb bob that provides a reference vertical line in the camera view. The quasi-static growth of the pendant droplet, which took around 80 minutes, was video-recorded. After extracting snapshots (bitmap image files, viz. BMP file format) from the video, the tilted images were rotated to align with the vertical line of the plumb bob (i.e., the true axis of symmetry for the

droplet profile) prior to the profile analysis. A larger droplet elongates more by gravity and fills the picture frame fully, providing a droplet profile with more pixels and improving the measurement accuracy. For our case, the capillary diameter to maximize the number of pixels on the droplet profile in the picture frame of our USB camera was calculated to range between 0.72 mm and 2.44 mm for surface tension between 501 mN/m and 718 mN/m [11, 12], respectively. Instead of the stainless-steel needle used in the contact angle measurement, we chose a glass capillary for the pendant drop method because of its availability in the above desired diameter and its transparency that allows observation of the meniscus movement inside the capillary. Recalling that Galinstan® is nonwetting on glass, i.e., it does not spread on the glass surface outside the capillary, the diameter calculated above should be the inner diameter of the capillary; we chose 1.22 mm for our measurements.

E. Electrowetting-on-Dielectric (EWOD)

The wetting conditions of a liquid on a solid can be modulated by various methods. In general, external energy (e.g. electrical, thermal) enters the system and calls for a configuration that would minimize the total energy. Among electrical methods, the mechanism of EWOD has been widely adopted, as illustrated in Fig. 4. Relations between the applied voltage and the resulting contact angle is described by the Lippmann-Young equation [20]

$$\cos\theta = \cos\theta_0 + \frac{1}{2\gamma} cV^2 \tag{5}$$

in which V is the voltage applied across the dielectric layer (between the liquid and the conductor underneath the dielectric), c is the capacitance per unit area of the dielectric, θ_0 is the initial contact angle without voltage applied, and θ is the contact angle when applying V.

Hermetic feedthrough enabled EWOD tests of Galinstan® inside the glove box while placing other apparatuses, e.g. the DC power source (Keithley 2425) and the amplifier (Trek PZD700), outside the glove box. We chose to use a tungsten probe tip for its chemical inertness with Galinstan® to electrically connect the droplet and the power source. Note that the synchronization of electrical activation and snapshots in our experiment allowed us to quickly capture the droplet spreading and minimize the effect of dielectric charging by reducing the total application of high voltages to less than one minute.

IV. RESULTS AND DISCUSSION

A. Contact Angle Measurements

Results of contact angle measurements of Galinstan® on different solid surfaces are summarized in Table IV along with the roughness information of the surfaces obtained by AFM measurements. The contact angles were calculated with sub-pixel accuracy [21]. The roughness

was quantified by different parameters interpreting the vertical deviations of the roughness profile from the mean line: R_q being the root mean square of the deviations; R_a being the arithmetic average of the absolute values; $R_{\max}$ being the maximum difference between the peaks and valleys; and surface area ratio being the ratio between the increased surface area (due to the roughness) and the perfectly flat surface. Galinstan® was found nonwetting on all surfaces tested.

However, we found that, once Galinstan® gets oxidized, the oxide shell, though thin, sticks on the surface and gives the illusion that Galinstan® wets almost all materials. To emphasize the detrimental impact of oxidation on measuring the wetting properties of Galinstan®, we measured its advancing and receding contact angles on glass in ambient air (~20.9% oxygen) as well, as shown in Fig. 5. The experiment setup remained exactly the same except that the glove box was vented to air. For example, the oxide shell was pinned on the glass surface during receding until most of the Galinstan® liquid has been pumped back into the syringe, as shown in Fig. 5(b). Such pinning effect resulted in incorrect advancing and receding contact angles of 165° and 7°, in contrast to the accurate angles of 146.8° and 121.5°, respectively, in Table IV. The receding angle would have been even lower than 7°, if the measurement had not been ended prematurely by the liquid disconnection during the suction back.

The contact angle information of Galinstan® is rare at this point. Kocourek [11] reported that contact angle of Galinstan® on glass is 122° in air and 166° in 6% hydrochloric acid. Their result in air stays within the wide range we observed in air, i.e., 7° and 165°. However, a direct comparison is inadvisable, because Kocourek reported only one contact angle instead of advancing and receding angles, and did not provide additional information such as roughness of the glass surface and details of the measurement procedure.

B. Surface Tension Measurement

For our pendant drop measurement, one experiment consisted of the formation, quasi-static growth, and dropping of a droplet, taking about 90 minutes. Frames of every second over the quasi-static growth (~80 minutes), i.e. ~4800 pictures, were collected from the video recording and provided enough data for statistical analysis. All pictures were analyzed using a computer program written to follow Eqs. 1-4 [22]. In addition to the Canny edge detection algorithm used in [16], the Sobel edge detection algorithm was also used for comparison. Fig. 6(a) presents the surface tension results with box plots, a quick graphical approach to examine data without any assumption of the underlying statistical distribution, using the two algorithms. Note that multiple outliers might overlap together, giving the appearance of one outlier in the plots. To assess whether or not the data has an approximate normal distribution, the normal probability plot of the two sets of data are drawn in Fig. 7. Not only can we see that calculated results from the Sobel edge detection algorithm tend to be larger, they also deviate more from the normal distribution, which is commonly assumed as observational errors. This is understandable, considering an edge

is a human-defined perception; different definition (i.e. different edge detection algorithms) might lead to different results. It is commonly believed that the Sobel edge detection is more sensitive to noise and thus inaccurate when compared to Canny edge detection, which reduces the noise by smoothing the image [23]. Therefore, based on the distribution of the results in Fig. 7 and information in [23], we conclude that the results from Canny edge detection are more reliable and use them for discussions in the remainder of this report.

Following the procedures described above, we have obtained the surface tension of Galinstan® as 534.6±10.7 mN/m. Because oxidation affects the surface tension measurement, the reading would drift as a freshly formed pendant droplet gets oxidized over time. As shown in Fig. 8, the main data (in O_2 < 0.5 ppm) stayed constant, confirming that the obtained value was free of any oxidation effect. To compare, we have run a pair of controlled experiments in slightly higher oxygen levels (in O_2 ~ 20 ppm and 500 ppm), which clearly reveal the oxidation effect on the surface tension measurement. The scatters in the data were caused mostly by the shocks and vibrations from the environment not filtered out by the current vibration-isolation plate. Despite the excessive scatters in the data of 20 ppm oxygen during 10-15 minutes, the overall trend is still clear.

In the pendant drop method, the fact that the capillary tip shares the focal plane with the hanging drop due to axisymmetry allowed us to obtain scale factor without resorting to additional tools. In contrast, the sessile drop method has to use a separate "ruler" to obtain the scale factor, and a tiny mismatch between the focal plane of the "ruler" and that of the sessile drop will linearly bias the results of surface tension [24]. Accordingly, we believe the pendant drop method used in this report provides more accurate results than the sessile drop method in measuring surface tension. Our result (534.6 mN/m in nitrogen) is comparable to but different from that of Kocourek [11] (517 mN/m in air), who used a sessile drop method.

C. Response to EWOD Actuation

The result of EWOD actuation on Galinstan® is demonstrated in Fig. 9 with the inset explaining the device used for the test. The EWOD device was prepared by depositing a ~4500Å-thick silicon nitride on an ITO-coated glass substrate using PECVD, followed by spin coating a ~1700Å-thick Teflon® AF 1600. Experiment data shown in Fig. 9 represents a mean of five experiments, and the error bar indicates standard deviation (instead of the mean standard error in [16]) of the data. The EWOD actuation was confirmed; contact angles changed with applied voltage, following the Lippmann-Young equation (Eq. 5) very well until contact angle saturates. The EWOD testing of liquid-metals is not as easy as regular liquids, because their large surface tension and nonwetting nature make it difficult to insert the probe into the liquid-metal and form a stable electrical connection. The first few contact angles (V = 0-20 V) in our measurements were affected by contact angle hysteresis, because the droplet spread out slightly

during the insertion and receded back after the insertion of the tungsten probe tip, which is highly nonwetting to Galinstan®. Therefore, the theoretical curve in Fig. 9 was generated using the initial contact angle obtained without the probe tip (155.9°). Excluding the saturation region, a contact angle decrease of ~30° has been achieved by applying 90 V. Such a contact angle change was sufficient for MEMS applications, such as the microswitch developed in [8].

V. CONCLUSION

We have characterized the interfacial properties of Galinstan® that are important for the design of micro devices: contact angles and surface tension. We overcame the strong oxidation of Galinstan® by performing the entire experiments inside a glove box of high-purity inert environment; its droplets finally behaved like a typical liquid when the levels of oxygen and moisture were brought down below 1 ppm (i.e., 0.0001%) and 0.5 ppm (i.e., 0.00005%), respectively. Signs of oxidation, such as color changes and gel-like behavior, was not found for more than 2 hours, providing us with sufficient time to measure contact angles and the surface tension of Galinstan®. The contact angles of Galinstan® were measured by sessile droplets on several materials commonly used in MEMS devices, and the surface roughness of the materials was also reported. For example, advancing and receding contact angles of Galinstan® on glass were measured to be 146.8° and 121.5°, respectively. In comparison, we also tested the contact angles in ambient air and confirmed that the illusion of Galinstan® wetting solid surfaces, including glass, was caused by the oxide skin sticking on the surfaces. The surface tension of Galinstan® was measured to be 534.6±10.7 mN/m, using a pendant drop method. In addition, the EWOD actuation of oxide-free Galinstan® was tested and found matching the Lippmann-Young equation. As a high level hermetic packaging of MEMS devices becomes available to prevent oxidation, Galinstan® is expected to eventually substitute mercury for microscale applications.

ACKNOWLEDGEMENTS

This work was supported by DARPA HERMIT program. The authors would like to thank Mr. Zhiyu Chen and Mr. Supin Chen for the fabrication of the devices and Mr. James Jenkins for the assistance on experiments in the glove box. Cogebi Inc. generously provided free mica samples.

REFERENCES

[1] Geratherm Medical AG (2011, July 20). *Galinstan Safety Data Sheet* [Online]. Available: http://www.rgmd.com/msds/msds.pdf

[2] CRC Press Online (2011, October 12). *CRC Handbook of Chemistry and Physics, 92nd Ed.* [Online]. Available: http://www.hbcpnetbase.com/

[3] A. S. F. Gerald, "Mercury relay," U.S. Patent 1773036, Aug. 12, 1930.
[4] A. H. Fleitman and J. R. Weeks, "Mercury as a nuclear coolant," *Nuclear Engineering and Design,* vol. 16, pp. 266-278, 1971.
[5] R. Clampitt and D. K. Jefferies, "Miniature ion sources for analytical instruments," *Nuclear Instruments and Methods,* vol. 149, pp. 739-742, 1978.
[6] A. Cao, P. Yuen, and L. Lin, "Microrelays With Bidirectional Electrothermal Electromagnetic Actuators and Liquid Metal Wetted Contacts," *Journal of Microelectromechanical Systems,* vol. 16, pp. 700-708, 2007.
[7] K. A. Shaikh, S. Li, and C. Liu, "Development of a Latchable Microvalve Employing a Low-Melting-Temperature Metal Alloy," *Journal of Microelectromechanical Systems,* vol. 17, pp. 1195-1203, 2008.
[8] P. Sen and C.-J. Kim, "A Fast Liquid-Metal Droplet Microswitch Using EWOD-Driven Contact-Line Sliding," *Journal of Microelectromechanical Systems,* vol. 18, pp. 174-185, 2009.
[9] P. Sen and C.-J. Kim, "A Liquid–Solid Direct Contact Low-Loss RF Micro Switch," *Journal of Microelectromechanical Systems,* vol. 18, pp. 990-997, 2009.
[10] T. D. Truong, "Selective Deposition of Micro Scale Liquid Gallium Alloy Droplets," MS Thesis, Mechanical and Aerospace Engineering Department, University of California (UCLA), Los Angeles, 2000.
[11] V. Kocourek, *Elektromagnetisches Abstützen von Flüssigmetall-Tropfen*, Ilmenau University of Technology Library, Germany, 2007.
[12] V. Kocourek, C. Karcher, M. Conrath, and D. Schulze, "Stability of liquid metal drops affected by a high-frequency magnetic field," *Physical Review E,* vol. 74, pp. 026303 1-7, 2006.
[13] A. W. Adamson and A. P. Gast, *Physical Chemistry of Surfaces*, 6th ed. New York: Wiley, 1997, ch. 2, pp. 4-47.
[14] S.-Y. Lin, L.-J. Chen, J.-W. Xyu, and W.-J. Wang, "An Examination on the Accuracy of Interfacial Tension Measurement from Pendant Drop Profiles," *Langmuir,* vol. 11, pp. 4159-4166, 1995.
[15] J. M. Andreas, E. A. Hauser, and W. B. Tucker, "Boundary Tension by Pendant Drops," *Journal of Physical Chemistry,* vol. 42, pp. 1001-1019, 1938.
[16] T. Liu, P. Sen, and C.-J. Kim, "Characterization of liquid-metal Galinstan for droplet applications," in *Proc. IEEE Conf. MEMS*, Hong Kong, China, 2010, pp. 560-563.
[17] R. G. Burton and R. A. Burton, "Gallium alloy as lubricant for high current density brushes," *IEEE Transactions on Components, Hybrids, and Manufacturing Technology,* vol. 11, pp. 112-115, 1988.
[18] R. P. Woodward First Ten Angstroms Inc. (2011, July 20). *Contact Angle Measurements Using the Drop Shape Method* [Online]. Available: www.firsttenangstroms.com/pdfdocs/CAPaper.pdf
[19] R. N. Lyon, *Liquid-Metal Handbook*, 2nd ed. Washington, D.C.: Atomic Energy Commission, Dept. of the Navy, 1952, ch. 4, pp. 170-171.
[20] J. Lee, H. Moon, J. Fowler, T. Schoellhammer, and C.-J. Kim, "Electrowetting and electrowetting-on-dielectric for microscale liquid handling," *Sensors and Actuators, A,* vol. 95, pp. 259-268, 2002.

[21] P. Sen, "Driving Liquid-Metal Droplets for RF Microswitches," PhD Thesis, Mechanical and Aerospace Engineering Department, University of California (UCLA), Los Angeles, CA, 2007.
[22] T. Liu, "Electromechanical Characteristics of Liquid-Metal Galinstan Droplets," BE Thesis, Electrical Engineering Department, Zhejiang University, Hangzhou, China, 2009.
[23] M. Sharifi, M. Fathy, and M. T. Mahmoudi, "A classified and comparative study of edge detection algorithms," in *Proc. Int. Conf. on Inform. Technology: Coding and Computing*, Las Vegas, USA, 2002, pp. 117-120.
[24] J. N. Butler and B. H. Bloom, "A curve-fitting method for calculating interfacial tension from the shape of a sessile drop," *Surface Science,* vol. 4, pp. 1-17, 1966.

BIOGRAPHIES

Tingyi "Leo" Liu received the B.Eng. degree in electrical engineering (with honors) from Zhejiang University, Hangzhou China, in 2009. He is currently working toward the Ph.D. degree in mechanical engineering at the University of California, Los Angeles (UCLA). Working in the Micro and Nano Manufacturing Laboratory, UCLA, his research interests include engineering designs utilizing capillarity, liquid-metal based micro devices, and micro gyroscope systems.

Prosenjit Sen was born in Calcutta, India in 1978. He received his Ph.D. degree in Mechanical Engineering from University of California, Los Angeles (UCLA) in 2007. He received his B.Tech. degree in Manufacturing Science and Engineering from Indian Institute of Technology, Kharagpur, India in 2000.

At the Micro and Nano Manufacturing Laboratory of UCLA, his research interests included microfluidic systems, droplet dynamics, liquid-metal based RF MEMS and reliability of electrowetting-on-dielectric (EWOD) devices. He has recently joined Innovative Micro Technology (IMT) in Santa Barbara, CA. Dr. Sen is recipient of Institute Silver Medal at Indian Institute of Technology, Kharagpur.

Chang-Jin "CJ" Kim (S'89–M'91) received the B.S. degree from Seoul National University, Seoul, Korea, the M.S. degree from Iowa State University, Ames, and the Ph.D. degree from the University of California, Berkeley, in 1991, all in mechanical engineering.

Since joining the faculty at the University of California, Los Angeles (UCLA), in 1993, he has developed several microelectromechanical-system (MEMS) courses and established a MEMS Ph.D. major field in the Mechanical and Aerospace Engineering Department in 1997. Directing the Micro and Nano Manufacturing Laboratory, he is also a founding member of the California NanoSystems Institute (CNSI) at UCLA. His research interests are in MEMS and nanotechnology, including design and fabrication of micro/nano structures, actuators, and systems, with a focus on the use of surface tension.

Prof. Kim has served on numerous technical committees and panels, including Transducers, the IEEE International Conference on MEMS, and the National Academies Panel on Benchmarking the Research Competitiveness of the U.S. in Mechanical Engineering. He is currently serving on the Editorial Advisory Board for the IEEJ Transactions on Electrical and Electronic Engineering and the Editorial Board for the Journal of Microelectromechanical Systems. A fellow of ASME, he was the recipient of the Graduate Research Excellence Award from Iowa State University, the 1995 TRW Outstanding Young Teacher Award, the 1997 NSF CAREER Award, the 2002 ALA Achievement Award, and the 2008 Samueli Outstanding Teaching Award. He has also been active in the commercial sector as a board member, scientific advisor, consultant, and founder of start-up companies.

TABLE I
COMPARISONS OF PROPERTIES OF GALINSTAN® AND MERCURY

Property	Galinstan® [1]	Mercury [2]
Color	Silver	Silver
Odor	Odorless	Odorless
Boiling point	> 1300°C	356.62°C
Melting point	-19°C	-38.83°C
Vapor pressure	$<10^{-6}$ Pa at 500°C	0.1713 Pa at 20°C
Density	6440 kg/m^3	13533.6 kg/m^3
Solubility	Insoluble	Insoluble
Viscosity	2.4×10^{-3} Pa•s at 20°C	1.526×10^{-3} Pa•s at 25°C
Thermal conductivity	16.5 W•m^{-1}•K^{-1}	8.541 W•m^{-1}•K^{-1}
Electrical Conductivity	2.30×10^{6} S/m	1.04×10^{6} S/m

TABLE II
BEHAVIOR OF GALINSTAN® DROPLET AT DIFFERENT OXYGEN TRACE LEVELS

Oxygen	Observation
0.2-20.9%	Droplet is distinctively non-spherical by instantaneous surface oxidation even at the moment of dispensing
~20 ppm	Droplet is spherical Droplet behaves like gel rather than true liquid
<1 ppm	Droplet behaves like true liquid
<0.5 ppm	Droplet behaves like true liquid The condition for all data in this report

TABLE III
SURFACE PREPARATION OF DIFFERENT MATERIALS TESTED FOR CONTACT ANGLES

Type	Material	Thickness	Preparation Method
Conductor	Tungsten	200 nm	Sputtered on silicon wafer
Insulator	Silicon nitride	1 μm	Low-stress LPCVD on silicon wafer
	Glass	1 mm	Degreased soda-lime microscope slide (Fisherfinest®)
Polymer	Parylene	1 μm	Vapor deposition on microscope slide
	Teflon®	560 nm	Spin-coated on PECVD silicon nitride on ITO-coated glass
Mica	Phlogopite	500 μm	Cleaved from its natural form provided by Cogebi, Inc.
	Muscovite	400 μm	Cleaved from its natural form provided by Cogebi, Inc.

TABLE IV
CONTACT ANGLES OF GALINSTAN® ON DIFFERENT MATERIALS

Type	Material	Contact Angles			Surface Roughness			
		θ_a/°	θ_r/°	$(\theta_a-\theta_r)$/°	R_q/nm	R_a/nm	R_{max}/nm	Surfaces Area Ratio
Conductor	Tungsten	161.3	119.6	41.7	3.31	2.54	27.27	0.13%
Insulator	Silicon nitride	147.0	126.1	20.9	1.38	1.09	13.43	0.37%
	Glass	146.8	121.5	25.3	2.05	1.38	30.2	0.30%
Polymer	Parylene	146.3	112.6	33.7	13.48	9.02	105.37	0.85%
	Teflon®	161.2	144.4	16.8	2.04	1.62	21.03	0.59%
Mica	Phlogopite	148.0	124.5	23.5	1.97	1.59	13.57	0.23%
	Muscovite	163.6	148.1	15.5	1.02	0.82	7.64	0.11%

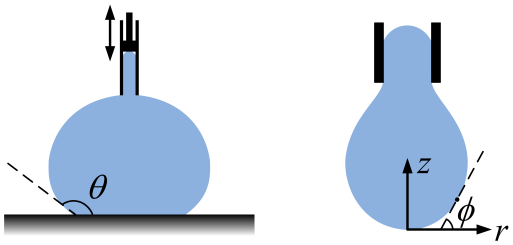

(a) (b)

Fig. 1. Measurements of contact angles and surface tension in this report. (a) Advancing and receding contact angles are measured by adding or subtracting volume to or from the sessile drop via the top needle until the contact line starts to move. (b) Surface tension is measured by pendant drop method using the cylindrical coordinate shown.

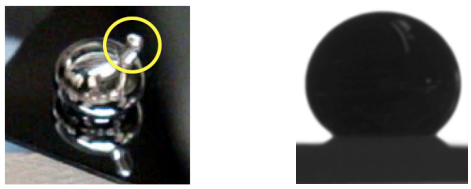

(a) (b)

Fig. 2. Oxidation effect on a Galinstan® droplet: (a) Angled view of a Galinstan® droplet (~2 mm in diameter) oxidized while being dispensed from a pipette (in less than 0.25 s), forming a non-spherical shape (i.e. the hornlike shape marked with a circle), even when the oxygen content was only ~0.2%; (b) Side view of a Galinstan® droplet (~1.5 mm in diameter) that formed a spherical shape and behaved as a liquid, only when the oxygen content was kept below 1 ppm.

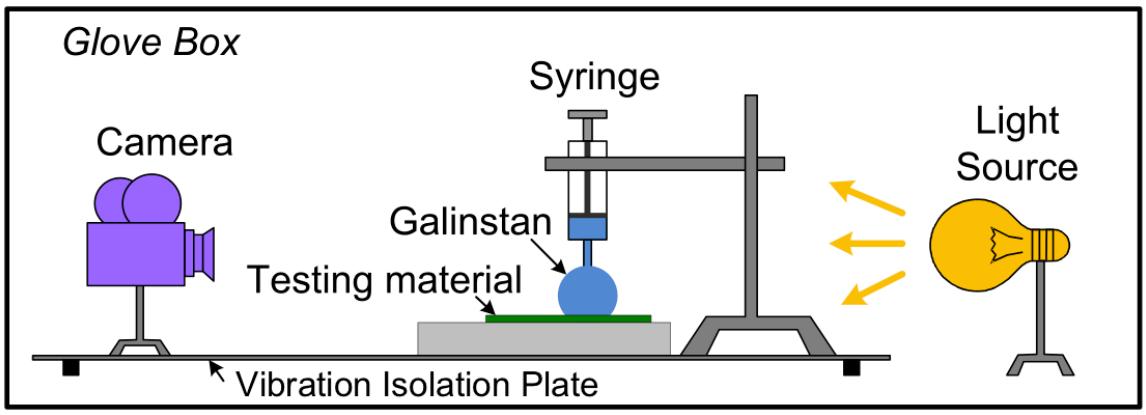

Fig. 3. Schematic of the experimental setup in a nitrogen-filled glove box, drawn for the measurement of contact angles on a sessile droplet. To measure the surface tension with a pendant drop, the testing material and its base substrate were removed, and a plumb bob was added.

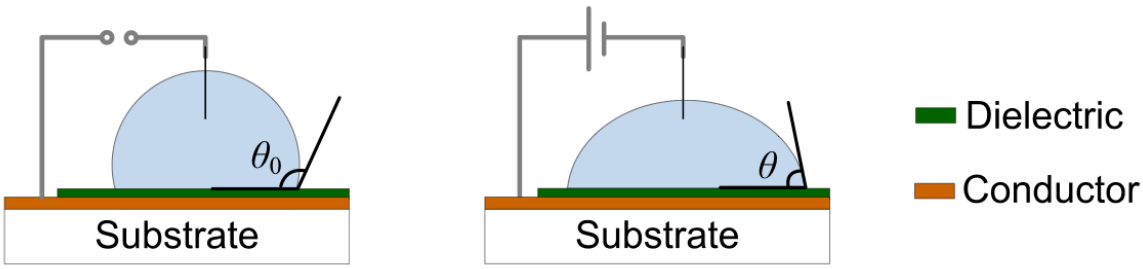

Fig. 4. EWOD actuation of a sessile liquid droplet

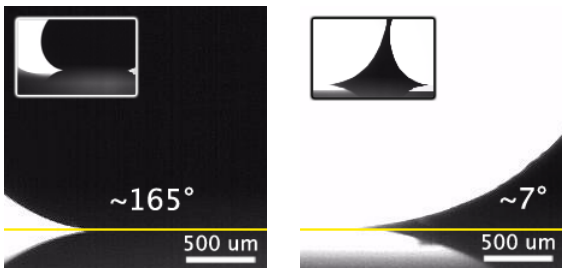

(a) (b)

Fig. 5. Three-phase contact regions of Galinstan® on a glass in ambient air (~20.9% oxygen): (a) advancing angle and (b) near receding angle. Pinning of the oxide skin makes the receding angle appear very low. Both (a) and (b) include an inset showing the larger field of view. The measurement of receding contact angle ended prematurely when the droplet was separated from the top needle.

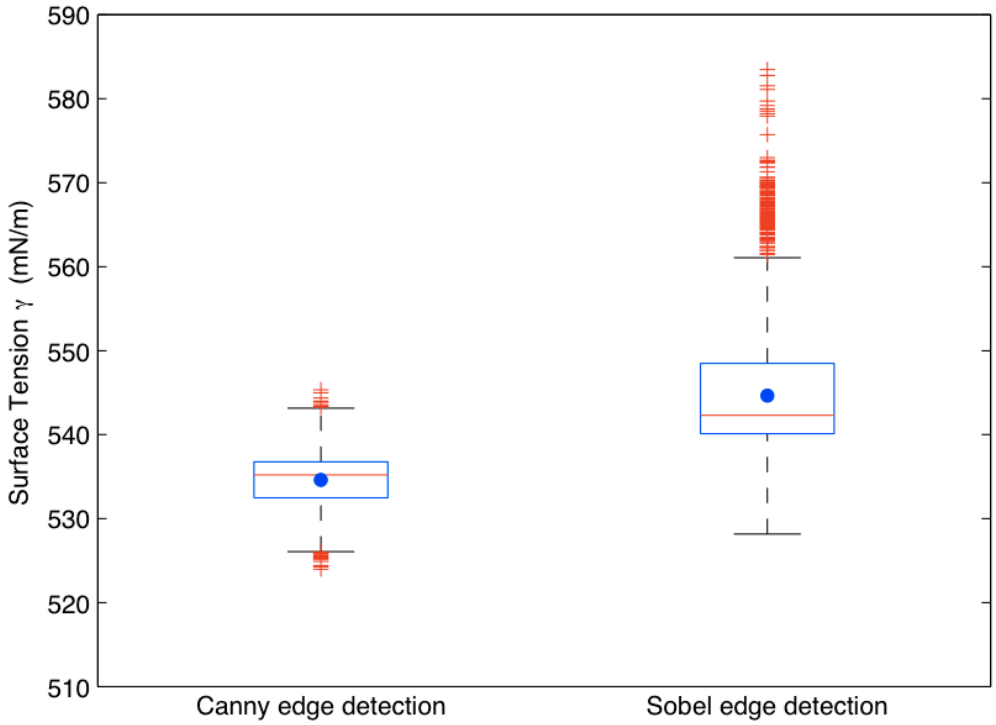

(a)

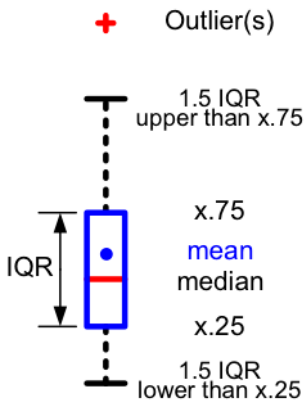

(b)

Fig. 6. Surface tension data of Galinstan® obtained. (a) Box plot of the surface tension measured by two edge-detection algorithms. (b) Meaning of the box plot. Interquartile range (IQR) excludes the highest and lowest 25% of data.

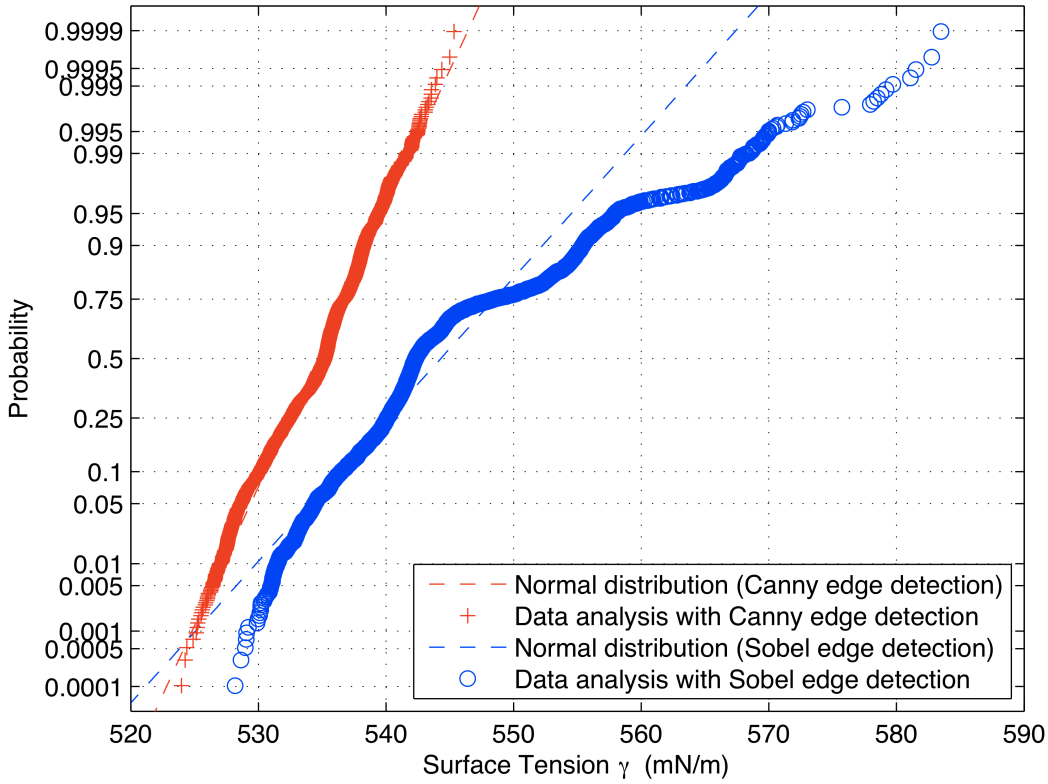

Fig. 7. The normal probability plots of the Galinstan® surface tension measured by two edge detection algorithms. The standard deviations of Canny algorithm and Sobel algorithm are 3.2093 mN/m and 7.7184 mN/m, respectively

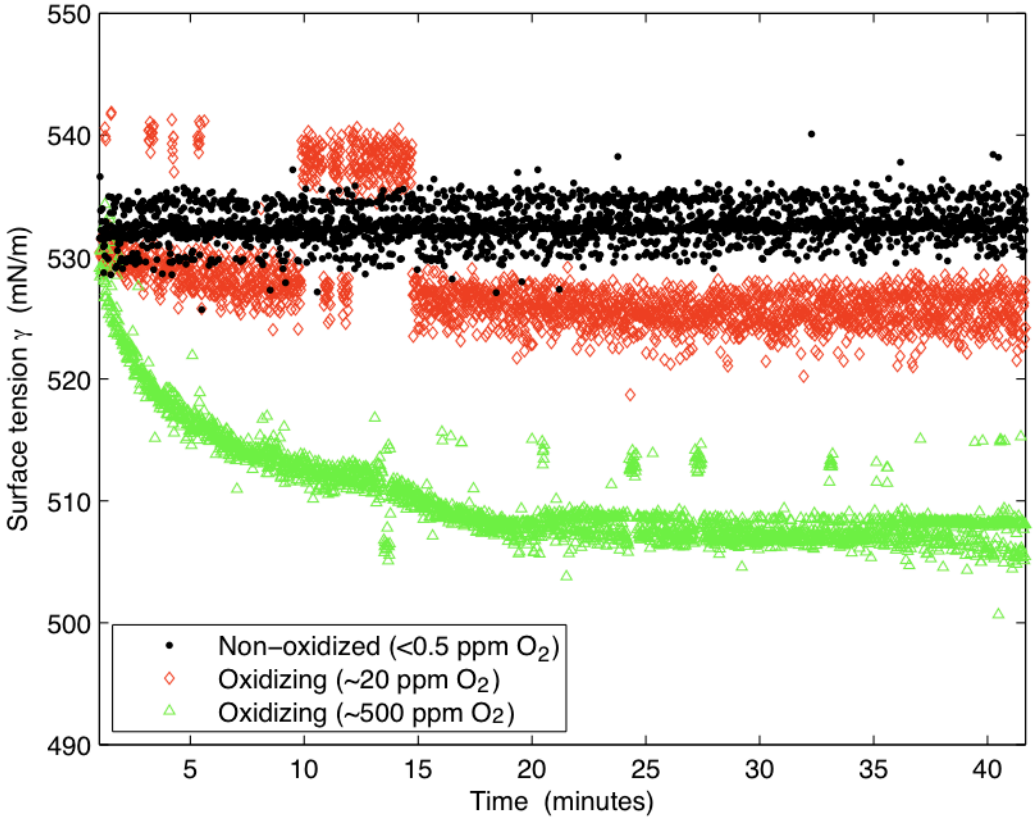

Fig. 8. Surface tension of Galinstan® measured during the first 40 minutes of the quasi-static droplet growth. Canny edge detection algorithm was used for calculation of surface tension every second. The surface tension in this report (solid black circles for $O_2 < 0.5$ ppm) displays virtually constant values, showing no effect of oxidation. In contrast, the values in two slightly oxidizing conditions (red hollow diamonds for $O_2 \sim 20$ ppm; green hollow triangles for $O_2 \sim 500$ ppm) show the effect of oxidation before the measurements were completed.

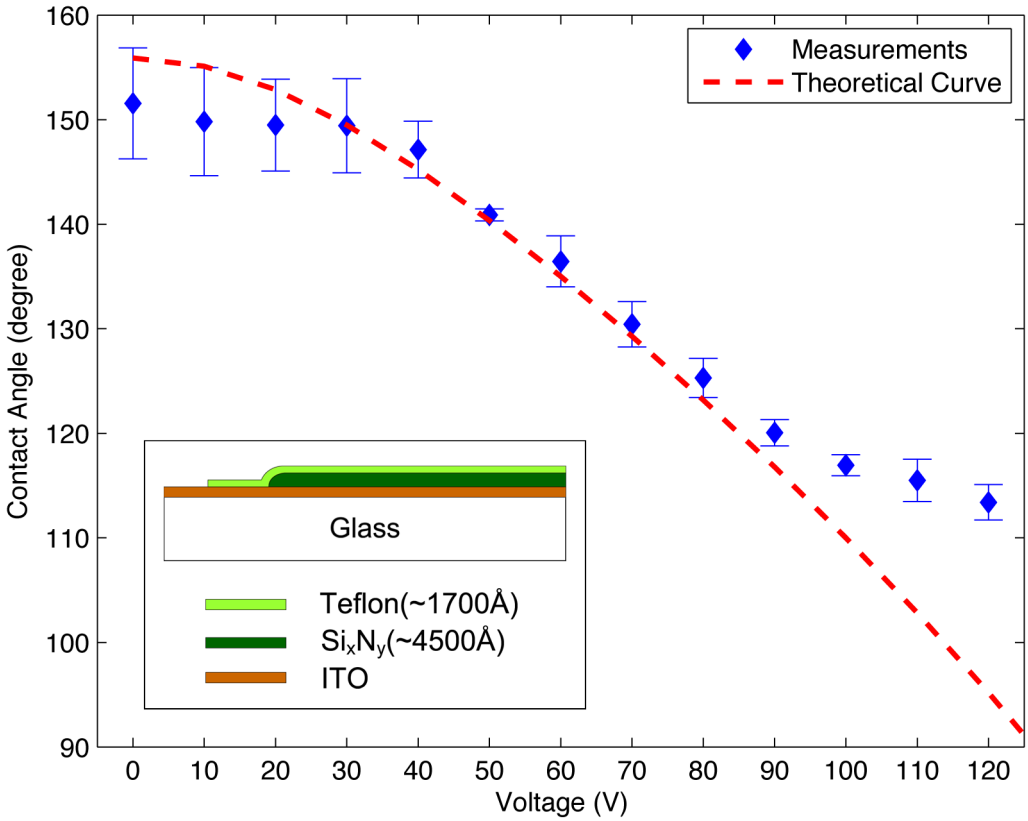

Fig. 9. Response of Galinstan® to EWOD actuation. The theoretical curve was drawn using the initial contact angle measured without a probe tip connection (155.9°) and the surface tension obtained in this report (534.6 mN/m). The total capacitance (per unit area) of the dielectric layers (Teflon® in series with silicon nitride) was calculated to be ~61 μF/m^2. The inset shows the device configuration used for the EWOD test.